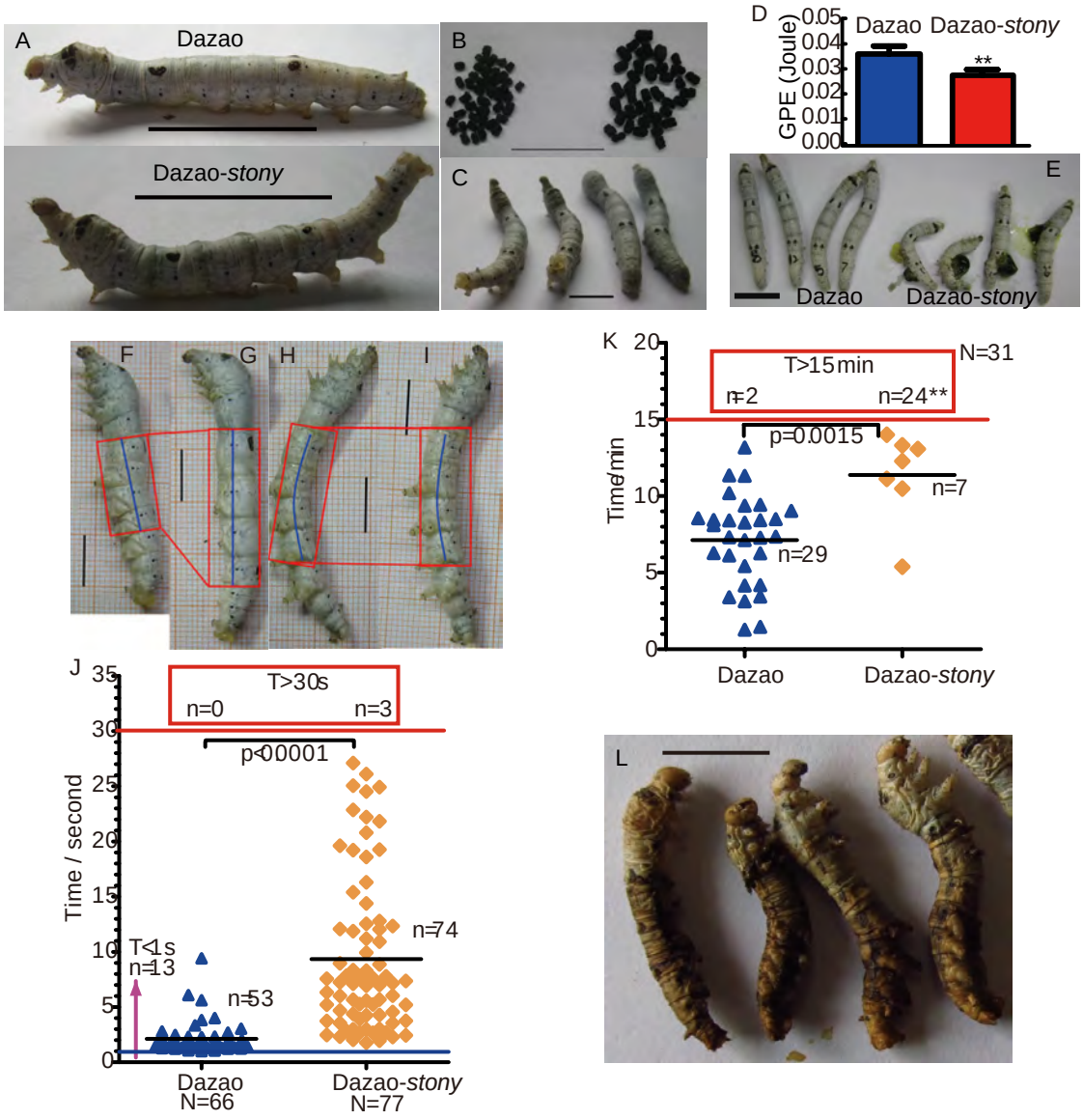

Figure S1 Additional phenotype and behavior assays of *stony* mutant. A. represents the phenotypes of the sides of Dazao and Dazao-*stony*, respectively. Scale bar: 2cm. B. Phenotypes of the excrement of Dazao and Dazao-*stony*. Scale bar: 2 cm. C. Rectocele phenomenon of Dazao-*stony*. Scale bar: 1 cm. D. Average of the GPE (gravitational potential energy) of Dazao and Dazao-*stony* strains selected for the dropping experiment, h=2m, (n=20). Data represent mean values ± S.D. Student's t test, ** $p<0.01$. E. Body rupture of Dazao-*stony* in the dropping experiment. Scale bar: 1 cm. F and H represent the phenotypes of Dazao and Dazao-*stony* injected with air, respectively. Scale bar: 1 cm. G and I represent the phenotypes of stretched individuals in F and H , respectively. Scale bar: 1 cm. The red box includes the abdomen segments (2^{nd} to 5^{th}) and the blue line represents length. J. Comparative inversion tests on Dazao and Dazao-*stony*. Both red and blue lines represent threshold time. The numbers in the red box indicate individuals which cannot turn over in 30 s The time of turning over in Dazao was significantly lower than that in Dazao-*stony* within the set time-frame (30 s). Mann-Whitney *U*-test. $P<0.0001$. K. crawling ability test under food inducement. The red line represents the threshold time. The numbers in the red box indicate individuals which cannot touch mulberry leaves in 15 min. ** represents $p<0.01$ χ^2-test. Compared to Dazao, Dazao-*stony* needed more time to touch mulberry leaves within the set time-frame (15 min). Mann-Whitney *U*-test. $P<0.0001$. Additionally, due to strong pressure in the body cavity, physical coordination of Dazao-*stony* was significantly poorer than that of Dazao during the crawling process (File S8). L. Phenotypes of *stony* mutants at the beginning of 5^{th} instar with molting difficulties. Scale bar: 1 cm.

Full-length cDNA of *BmorCPR3*

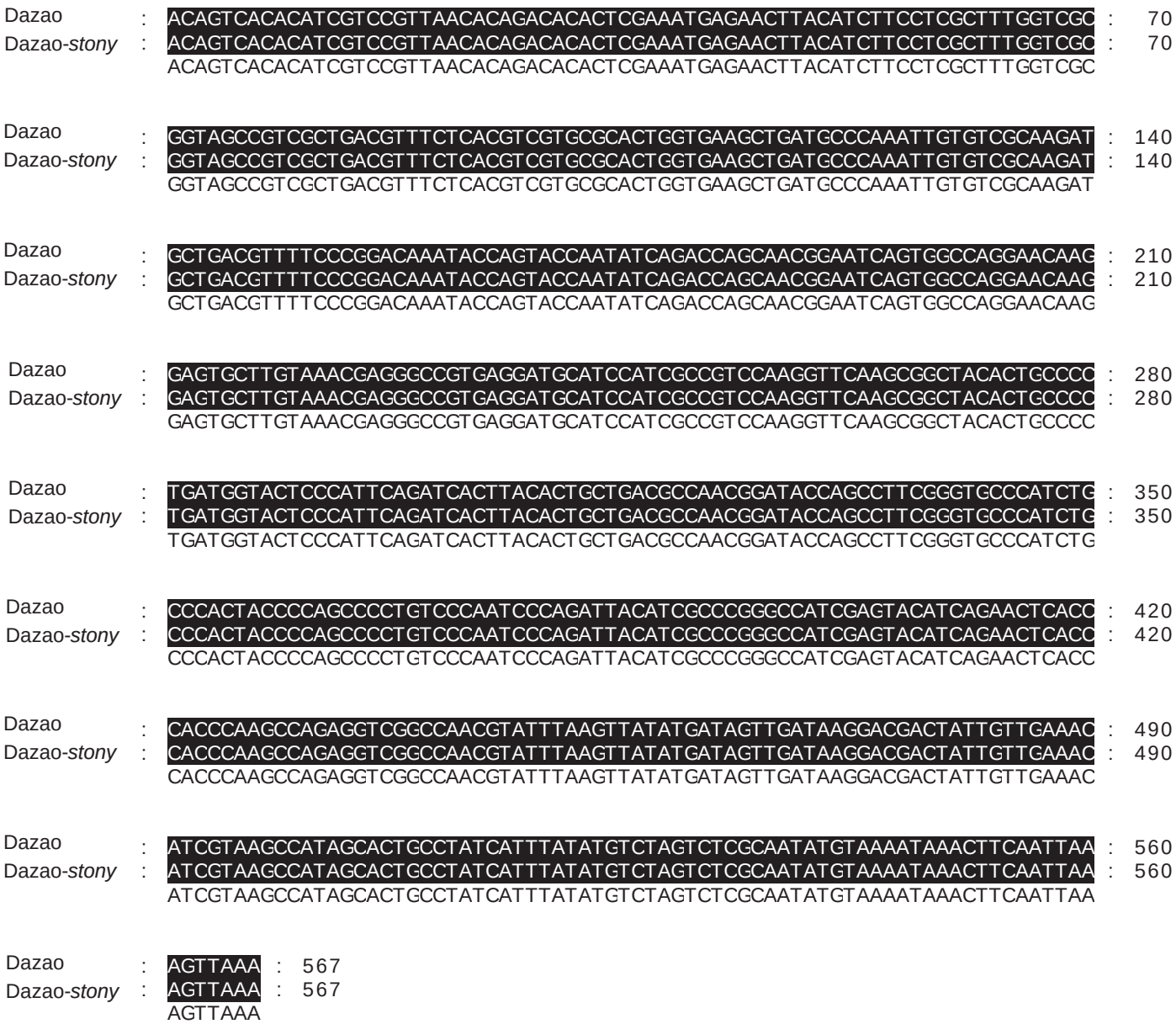

Figure S2 Full-length *BmorCPR3* cDNA sequences of Dazao and Dazao-*stony*.

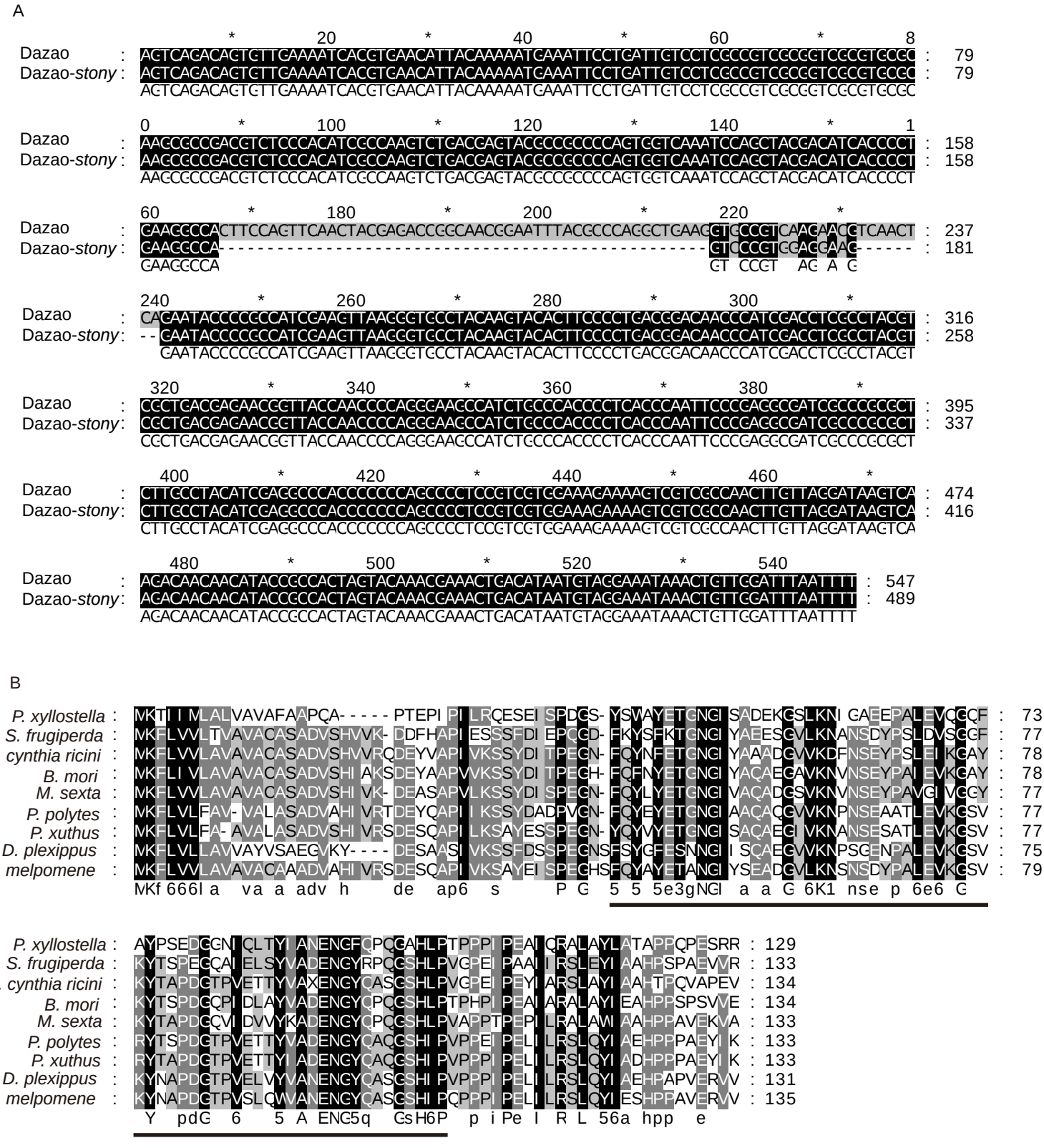

Figure S3 Sequence characteristics of *BmorCPR2* between Dazao and Dazao-*stony*. A. Full-length cDNA sequences of *BmorCPR2* between Dazao and Dazao-*stony*. B. Alignment of BmorCPR2 and orthologs among nine Lepidopera species. The orthologs were identified using BLAST (blastp and tblastn), known genomes or EST databases of selected Lepidopera insects, NCBI, CuticleDB (http://bioinformatics.biol.uoa.gr/cuticleDB and OrhtoDB (http://cegg.unige.ch/orthodb6). Sequence alignment using Muscle program (http://www.ebi.ac.uk/Tools/msa/muscle/), is listed as follows: *Bombyx mori* BmorCPR2, *Papilio polytes* CPR2, BAM18876.1, *Papilio xuthus* CPR2, BAG30800.1, *Danaus plexippus* EHJ77392.1, *Manduca sexta* Msex000162-RB, (Manduca base), *Heliconius melpomene* HMEL002550-PA, (Heliconius Genome Project), *Samia cynthia ricini* I10A02NGRL0007_H08 (SilkBase), *Plutella xylostella* Px003256.1 (Diamondback moth Genome Database), *Spodoptera frugiperda* Sf1P23819-5-1, (SPODOBASE). The black line represents the RR1 motif.

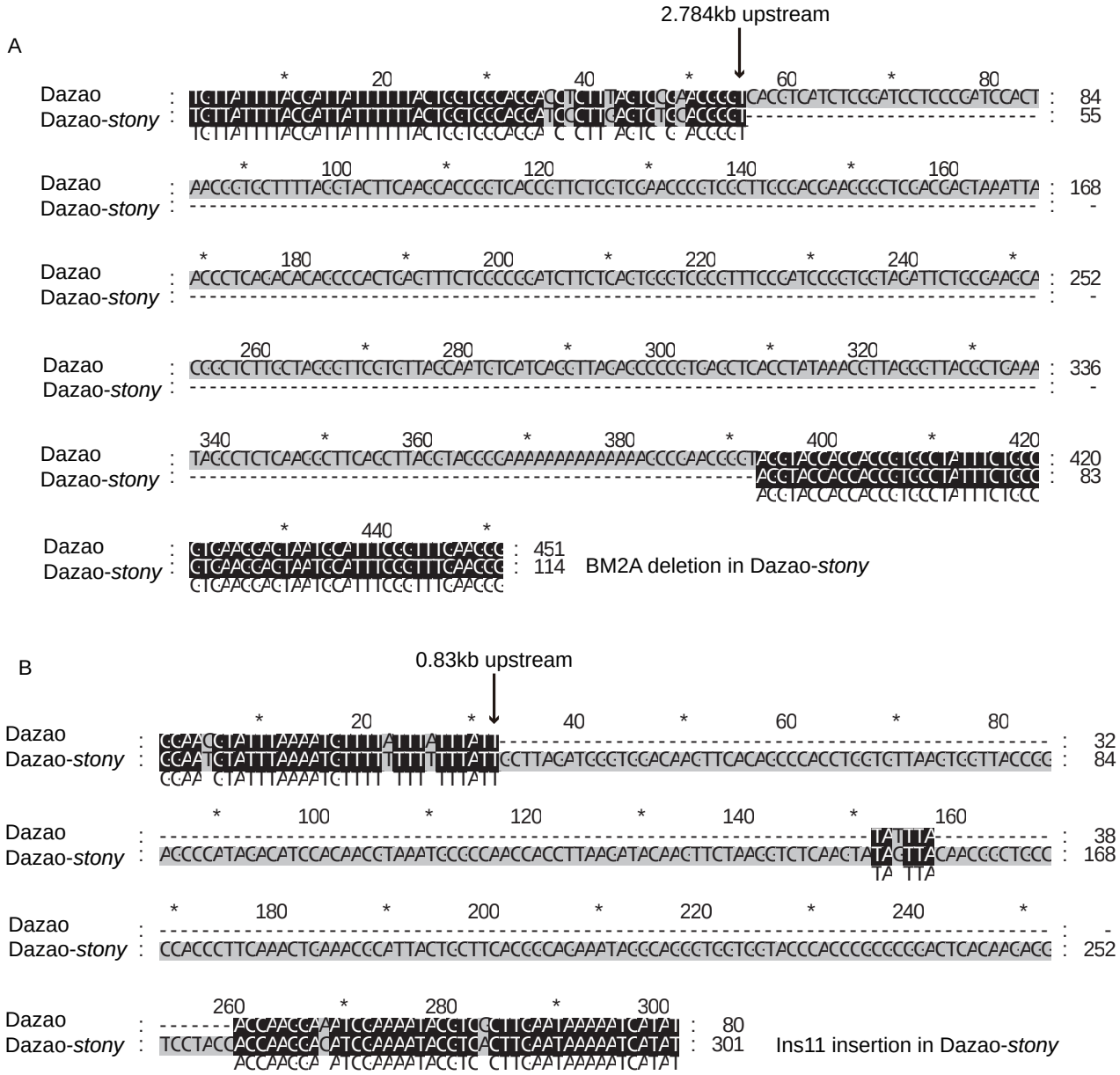

Figure S4 Comparison of the ~2.78 kb (A) and ~0.83 kb (B) upstream genomic sequences of *BmorCPR2* of Dazao and Dazao-*stony*.

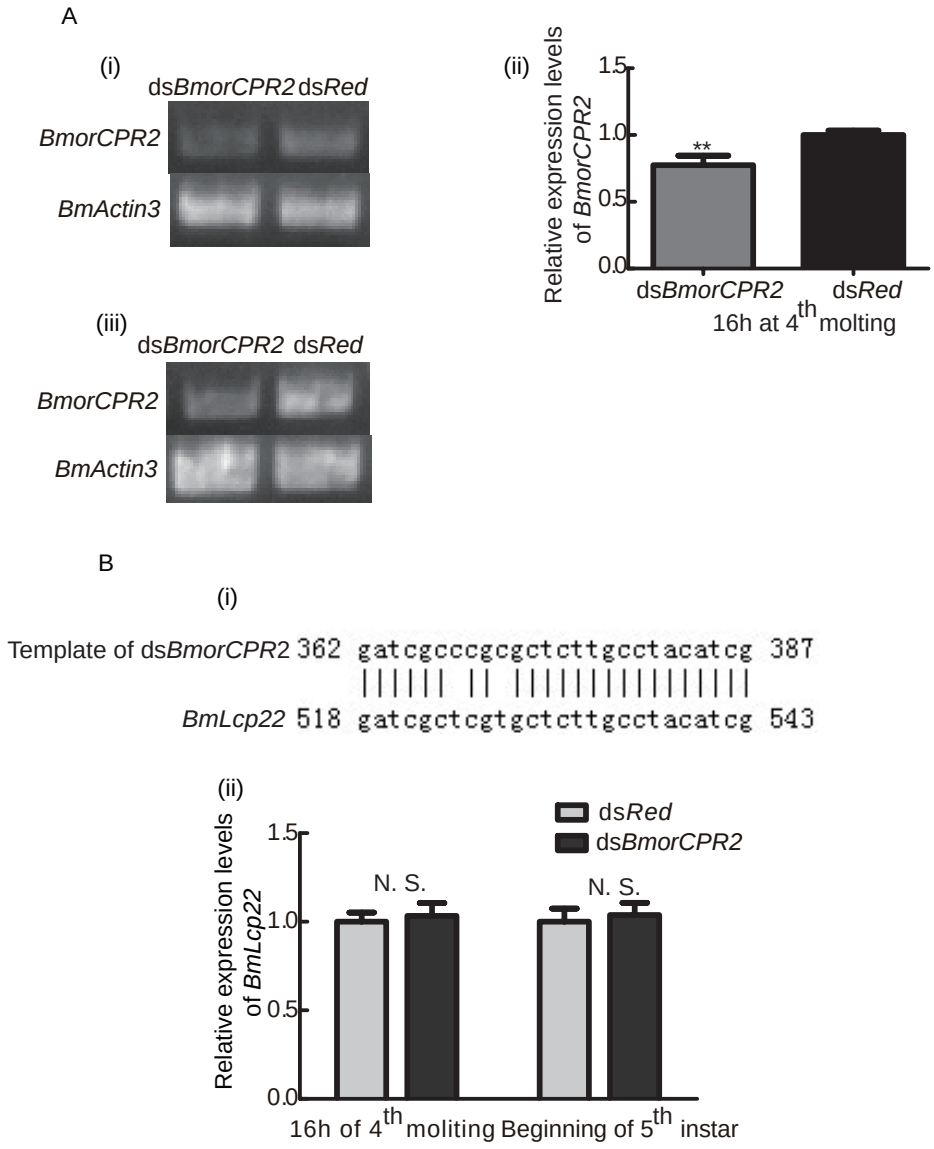

Figure S5 Analysis of the effects of RNAi. A. RT-PCR and qRT-PCR analysis. (i) and (ii) represent expression of *BmorCPR2* in larvae subjected to RNAi at 16 h of 4th molting. (iii) represent expression of *BmorCPR2* in larvae subjected to RNAi at beginning of 5th instar. B. Detection of RNAi off-target effects. (i) Nucleic acid alignment between *BmLcp22* and ds*BmorCPR2* template. (ii) Relative expression levels of *BmLcp22*. Data are presented as mean values ± S.D. N.S. indicates no significant differences in the *BmLcp22* expression levels between ds*BmorCPR2* and ds*Red* groups.

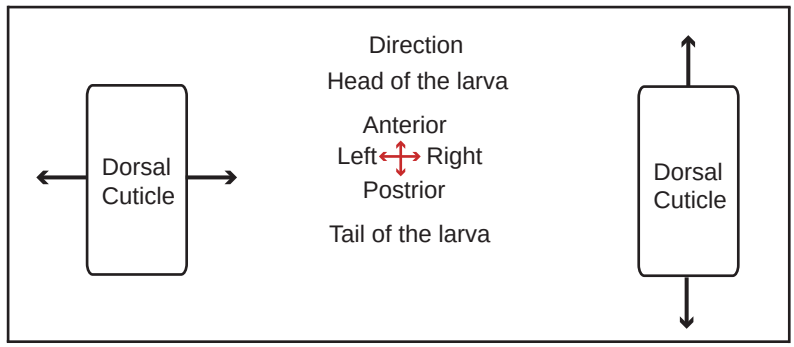

Figure S6 Schematic diagram of manipulation in the stretching test. Black arrowhead represents the stretching direction and red cross arrowhead indicates location.

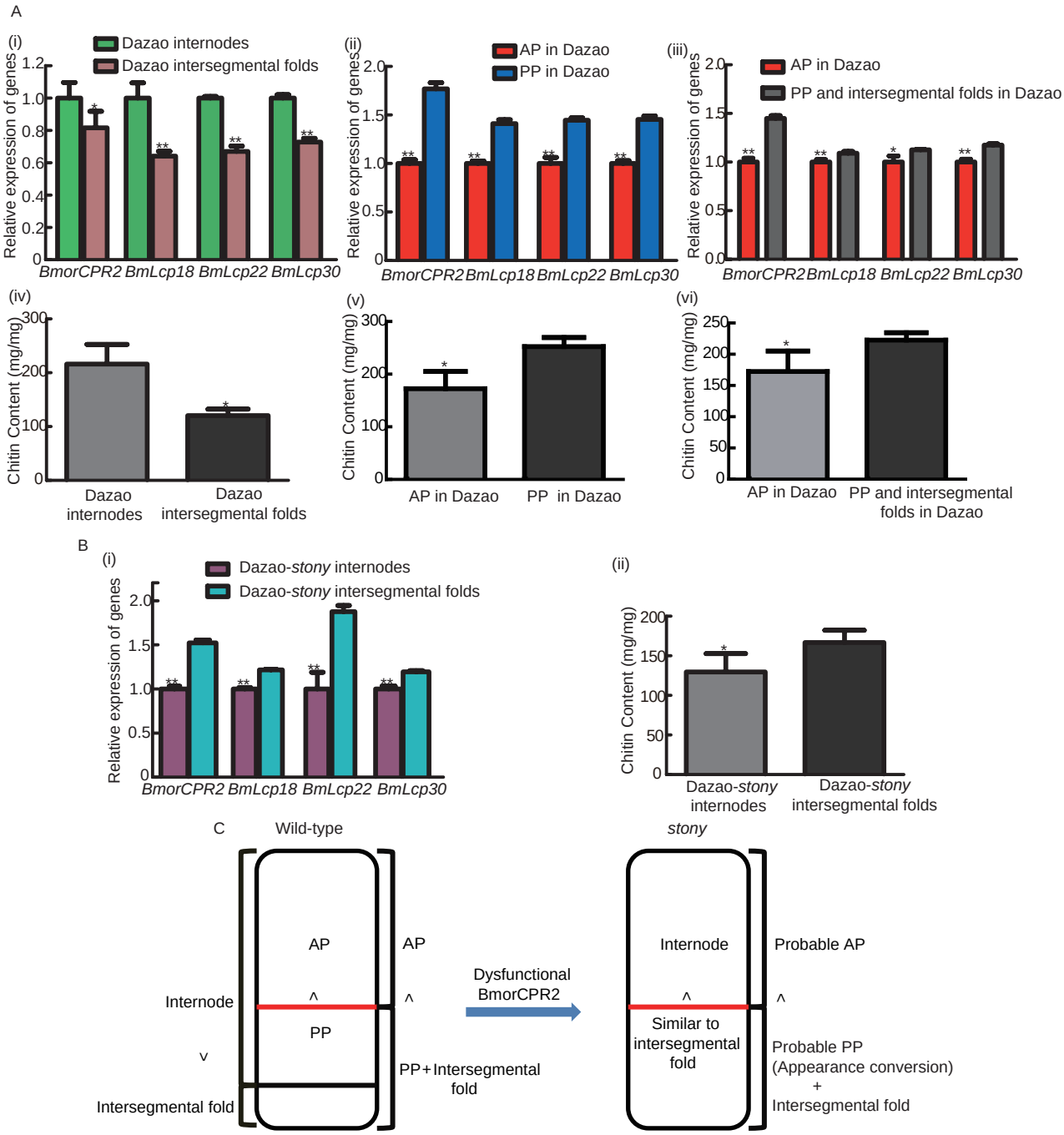

Figure S7 Detailed data of Gene expression profiles and chitin distribution in various parts of segmental cuticle in Dazao and Dazao-*stony*. A. Detailed data of cuticular gene expression profiles and chitin distribution in different parts of Dazao dorsal segment cuticle. (i) and (iv) represent gene expression profiles (n=3) and chitin content (n=4) of the internodes and intersegmental folds in Dazao, respectively. (ii) and (v) represent the gene expression profiles (n=3) and chitin content (n=3) of AP and PP in Dazao, respectively. (iii) and (vi) represent gene expression profiles (n=3) and chitin content (n=3) of the anterior and remaining parts (posterior parts and intersegmental folds) in Dazao, respectively. Data are presented as mean values ± S.D. Student's *t*-test, *represent $p<0.05$, **represents $p<0.01$. B. Detailed data of cuticular gene expression profiles and chitin quantification in different parts of Dazao-*stony* segment. (i) represents gene expression profiles (n=3) of internodes and intersegmental folds in Dazao-*stony*. Data are presented as mean values ± S.D. Student's *t*-test, ** represents $p<0.01$. (ii) represents the chitin content (n=4) of the internodes and variant intersegmental folds in Dazao-*stony*. Data are presented as mean values ± S.D. Student's *t*-test, *represents $p<0.05$. C. Derived schematic diagram for formation of the abnormal intersegmental fold in *stony* mutant. The black line represents the boundary of internode and intersegmental fold in Dazao. The red line represent the boundary of AP and PP. The tip of symbol '∧' and symbol '∨' point to the parts with lower genes expression and chitin content.

File S1

Supporting Methods

(a) Detailed operation of physiology test and behavior assays

In the dropping experiment, 20 Dazao-*stony* and Dazao individuals were subjected to a height of 2 m, followed by motion of a free falling body. The numbers of ruptured Dazao and Dazao-*stony* individuals were added up to compare their abilities to buffer the shock. To compare the flexibility and nesting ability of internode and intersegmental fold between Dazao and Dazao-*stony*, we injected 4 mL air into larvae, and stretch along the anterior-posterior axis of the body. To determine abdomen crooking ability, larvae were inverted to turn the dorsum down and the thorax pressed lightly to prevent writhing to the two sides. Subsequently, inversion towards the abdomen was observed. The number of individuals able to writhe to abdomen, time needed, and the angle between the dorsum and horizontal plane (performed using the digital camera, image J, and angle test software) were recorded. To determine grasping state and duration, larvae were placed on the middle of the mallet (diameter: ~0.9 and ~1.4 cm) in the larval grasping experiment. In the inversion assay analyzing dorsum crooking ability, we fixed the back of larvae on the plane carefully and unclamped them quickly to record the rolling state and time required. We additionally performed a food-inducing crawling experiment. Specifically, 5th instar day 5 larvae subjected to 10 h starvation were selected. Larvae were placed ~4 cm away from fresh mulberry leaves(Dethier 1941; Slifer 1955), and their crawling behavior and time to reach leaves recorded. In the phenotype analysis, physiology test and behavior assays, healthy Dazao and Dazao-*stony* larvae on day 5 of 5th instar glutted with mulberry leaf and subsequently starved for 4 h were selected, except for those used in the crawling experiment.

(b) Detailed operation of chitin binding

The soluble proteins extracted from sediment were dialyzed to eliminate SDS using Tang's method (TANG *et al.* 2010). Ethanol in mixed chitin beads was discarded and chitin resuspended with binding buffer (20 mM HEPES, 15 mM NaCl, pH 7.4). Next, ~100 μg cuticular protein of Dazao was mixed with chitin (volume ratio of 1:2, total volume 1 ml) in a 1.5 mL EP tube. The solution was incubated at 16°C for 4 h and shaken at 40 rpm. Following centrifugation (9000g, 4°C), the supernatant (S-incubation) was collected and added to 1.2 mL washing buffer (20 mM HEPES, 1 M NaCl, pH 7.4). Next, the mixture was shaken for 40 s and centrifuged under set conditions (9000g, 4°C). The supernatant was removed and the wash step repeated once. The final supernatant fraction (W2) and remaining chitin sediment were collected. S-incubation, W2 and chitin sediment were mixed with Laemmli sample buffer and heated at 95°C for 10 min, and the supernatant collected and analyzed using 15% SDS-PAGE.

(c) Detailed operation of LC-MS/MS

The gel was suspended in 200-400 μL decolorizing agent (30% ACN/100 mM NH4HCO3) until transparent, the supernatant was removed and frozen to dryness. Next, 100 mM DTT was added and incubated for 30 min under 56°C. After removal of the supernatant, 200 mM IAA was added, and the sample incubated in the dark for 20 min. The supernatant was removed and the sample treated with 100 mM NH4HCO3 at room temperature for 15 min. Following removal of the supernatant, ACN was added. After 5 min, the supernatant was blotted and frozen to dryness. Next, the dried sample was incubated overnight with 2.5-10 ng/μL Trypsin solution (37°C, about 20 h) and the enzymatic hydrolysate added to a new EP tube. We further added 100 μL extraction buffer（60%ACN/0.1%TFA）to the gel, followed by ultrasound for 15 min, combined with the enzymatic hydrolysate for freezing to dryness. The capillary performance liquid chromatography method was performed as follows: the chromatographic column was equilibrated with 95% solution A (0.1% formic acid), and the sample

loaded onto Trap column through an automatic sampler. Solution B (84% acetonitrile) flowthrough was as follows: 0-30 min with a linear gradient of 4 to 50%, 30-34 min with a linear gradient of 50 to 100%, and 34-40 min whereby the solution was maintained at 100%. The mass-charge ratios of peptide and peptide fragments were collected using the method for collecting MS2 scans after each full scan. Using BIOWORKS and SEQUEST programs, the raw file was searched in the related database (NCBI, http://silkworm.swu.edu.cn/silkdb/doc/download.html). Search steps were referenced to the procedure of Tang et al. (TANG *et al.* 2010).

Literature cited

DETHIER, V. G., 1941 The Function of the Antennal Receptors in Lepidopterous Larvae. Biological Bulletin **80:** 403-414.

SLIFER, E. H., 1955 The detection of odors and water vapor by grasshoppers (Orthoptera, Acrididae) and some new evidence concerning the sense organs which may be involved. Journal of Experimental Zoology **130:** 301-317.

TANG, L., J. LIANG, Z. ZHAN, Z. XIANG and N. HE, 2010 Identification of the chitin-binding proteins from the larval proteins of silkworm, Bombyx mori. Insect Biochem Mol Biol **40:** 228-234.

Files S2-S8

Available for download as AVI files at

http://www.genetics.org/lookup/suppl/doi:10.1534/genetics.113.158766/-/DC1

File S2 Video of dropping experiment

File S3 Video of abdominal crooking test

File S4 Video of grasping test on the large diameter mallets

File S5 Video of grasping test on the small diameter mallets

File S6 Video of inversion test with non hand-touch

File S7 Video of inversion test with hand-touch

File S8 Video of crawling ability test

Table S1 Primers used in this study

Available for download as an Excel file at http://www.genetics.org/lookup/suppl/doi:10.1534/genetics.113.158766/-/DC1

Table S2 LC-MS/MS identification in analysis of BmorCPR2 in target gels

Gel at ~15.3 kD	Protein requiring to be focused on	MW Charge	PI Rank	No. of unique peptids	UniquePepCount MH+	Sequence Coverage (%)	Peptide sequences	motif
Dazao-SDS PAGE	BmorCPR2	15270.2	5.06	5	1363.498	51.7	K.NVNSEYPAIEVK.G	RR-1
					1079.1851		K.SDEYAAPVVK.S	
					3295.4731		K.SSYDITPEGHFQFNYETGNGIYAQAEGAVK.N	
					1837.0688		R.ALAYIEAHPPSPSVVER.K	
					1965.2418		R.ALAYIEAHPPSPSVVERK.V	
Dazao-chitin binding	BmorCPR2	15270.2	5.06	3	1363.498	31.5	K.NVNSEYPAIEVK.G	RR-1
					1079.1851		K.SDEYAAPVVK.S	
					1837.0688		R.ALAYIEAHPPSPSVVER.K	
Dazao-*stony*-SDS PAGE	BmorCPR2	-[a]	-	-	-	-	-	-

[a] **undetected by LC-MS/MS**

Table S3 Statistic of RNAi

Treatment	Injected No.	No. of successful ecdysis	living and exhibiting RNAi phenotype	No. of Death during the molting stage
dsBmorCPR2	55	30	22	3
dsRed	43	41	0	2

Table S4 Amino acid identity of BmorCPR2 with its orthologs.

	B. mori	*P. polytes*	*P. xuthus*	*D. plexippus*	*M. sexta*	*H. melpomene*	*S. cynthia ricini*	*P. xyllostella*	*S. frugiperda*
B. mori	100%	59%	58%	57%	65%	55%	59%	54%	52%
P. polytes		100%	75%	58%	54%	58%	64%	40%	50%
P. xuthus			100%	60%	57%	64%	62%	47%	45%
D. plexippus				100%	51%	66%	58%	40%	46%
M. sexta					100%	58%	64%	50%	53%
H. melpomene						100%	54%	43%	44%
S. cynthia ricini							100%	45%	61%
P. xyllostella								100%	47%
S. frugiperda									100%